Proceedings of the ASME 2011 Conference on Smart Materials Adaptive Structures & Intelligent Systems
SMASIS 2011
September 18-21, 2011, Scottsdale, Arizona, USA

SMASIS2011/5008

NONLINEAR STOCHASTIC FEEDBACK CONTROLLERS FOR VIBRATORY ENERGY HARVESTERS WITH POWER FLOW CONSTRAINTS

Ian L. Cassidy*
Department of Civil & Environmental Engineering
Duke University
Durham, North Carolina 27708
Email: ian.cassidy@duke.edu

Jeffrey T. Scruggs
Department of Civil & Environmental Engineering
Duke University
Durham, North Carolina 27708
Email: jeff.scruggs@duke.edu

Sam Behrens
CSIRO Energy Centre
P.O. Box 330
Newcastle, New South Wales 2300
Australia
Email: sam.behrens@csiro.au

ABSTRACT

This study addresses the formulation of feedback controllers for stochastically-excited vibratory energy harvesters. Maximizing power generation from stochastic disturbances can be accomplished using LQG control theory, with the transducer current treated as the control input. For the case where the power flow direction is unconstrained, an electronic drive capable of extracting as well as delivering power to the transducer is required to implement the optimal controller. It is demonstrated that for stochastic disturbances characterized by second-order, bandpass-filtered white noise, energy harvesters can be passively tuned such that optimal stationary power generation only requires half of the system states for feedback in the active circuit. However, there are many applications where the implementation of a bi-directional power electronic drive is infeasible, due to the higher parasitic losses they must sustain. If the electronics are designed to be capable of only single-directional power flow (i.e., where the electronics are incapable of power injection), then these parasitics can be reduced significantly, which makes single-directional converters more appropriate at smaller power scales. The constraint on the directionality of power flow imposes a constraint on the feedback laws that can be implemented with such converters. In this paper, we present a sub-optimal nonlinear control design technique for this class of problems, which exhibits an analytically computable upper bound on average power generation.

INTRODUCTION

Electromechanical systems to harvest vibratory energy have been the subject of considerable research activity over the last decade, with the focus being primarily on low-power applications requiring energy-autonomy, such as wireless sensing and embedded computing systems [1–3]. A typical vibratory energy harvester relies on a passive electromechanical system, which consists of flexible mechanical structure with embedded transducers, to generate power from an exogenous disturbance. The transducers must be interfaced with a power electronic network that extracts power and delivers it to a storage device, such as a rechargeable battery or a supercapacitor.

The single-directional DC/DC converter in Figure 1 (a), and variants thereof, has gained a significant amount of attention for low-power energy harvesting applications [4–6]. This particular circuit is called a buck-boost converter due to the fact that it can make the output voltage magnitude less than or greater than the input voltage magnitude. Power flow in such converters is regulated via high-frequency pulse-width modulation (PWM) switching control of the MOSFETs in the circuitry. Single-directional DC/DC converters are advantageous in small-scale applications, because they only require that a single MOSFET be switched, thus reducing gating losses. However, for applications where the parasitic losses are small in comparison to the average power generated, the single-directional power flow capability of these converters can hamper their ability to optimize power generation from stochastic dynamical responses, as illustrated in [7].

In Ottman *et al.* [8], they experimentally demonstrated the operation of a buck converter to extract power from a piezoelectric transducer, and proposed that for such applications, it was advantageous to operate the converter in the discontinuous conduction regime. Subsequent studies for buck-boost converters in discontinuous conduction have been examined by Lefeuvre *et al.* [5] and later by Kong *et al.* [6]. In this regime, the in-

*Address all correspondence to this author.

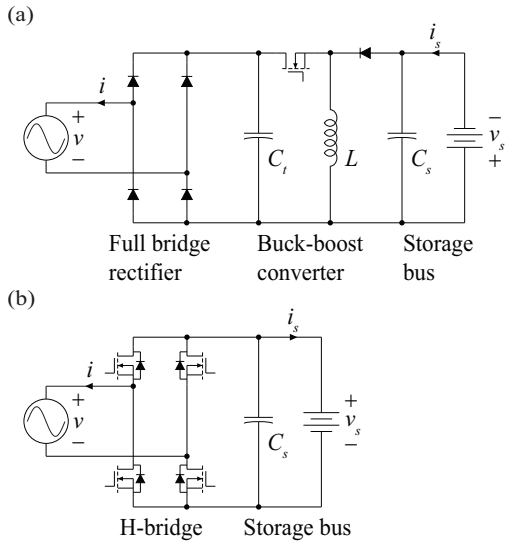

FIGURE 1. Energy harvesting converters interfaced with a storage bus: (a) full bridge rectifier connected to a buck-boost converter; (b) h-bridge.

ductor fully demagnetizes (i.e., its current drops to zero) before the end of the switching cycle, and remains so until the converter's MOSFET is gated on again at the leading edge of the next switching cycle. Operation of a buck-boost converter in discontinuous conduction results in an input admittance which is decoupled from the behavior of the storage voltage. Furthermore, if the transducer side capacitance, C_t, is sufficiently small, and possibly with supplemental input filtering, then the admittance is approximately linear and resistive in low- to mid-frequency bands, with the value of the effective resistance being proportional to the inverse-square of the switching duty cycle. As such, the design of these converters for optimal operation proceeds by first determining the effective shunt resistance which maximizes power generation from the transducer, and then synthesizing the duty cycle from this resistance.

For energy harvesting applications in which the disturbance is characterized by a single frequency, such converters can be incorporated into a larger passive network and can be tuned to optimize power generation. As pointed out in [7, 9], power generation is optimized by matching the input admittance of the effective passive network (including the effective resistance of the converter) to the complex conjugate transpose of the harvester admittance at this frequency. However, for cases in which the disturbance is modeled as a stochastic process, optimization of the dynamic behavior of the electronics for maximal power generation is more challenging. It has been shown in [7] that maximizing the power generated from an energy harvester using the same impedance matching techniques mentioned above, always results in an anti-causal admittance. That study also showed that an optimal causality-constrained admittance does exist, and that it can be determined using LQG control theory. Another approach for determining admittances for this class of problems has been proposed by Adhikari *et al.* [10], in which a Laplace-domain analysis is used to determine the analytical expression for the resistance that maximizes the mean power harvested.

For the stochastic case, Scruggs showed in [7] that if the electronics of energy conversion are efficient enough, then the optimal causal control of transducer current (as derived by LQG theory) cannot be realized with a passive network. This is because in such circumstances, there are frequency bands in which the average power for the optimized system flows the other way; i.e., from storage back into the harvester. That study advocates the realization of a synthetic dynamic admittance using a two-way (i.e., four-quadrant) power electronic converter. One example of such a converter, called an H-bridge, is shown in Figure 1 (b). Operation of the H-bridge requires control of four MOSFETs and thus requires more parasitic power than a one-directional converter, which is the price paid for two-way directionality of power flow. This type of drive has to be capable of high-bandwidth current tracking, and can be accomplished using hysteretic switching or PWM techniques [11].

For stochastic energy harvesting applications the theoretically-optimal power generation current is a feedback function of the system response, including the transducer voltage, as well as other response states that may be available via sensor feedback. Allowable complexity of this algorithm depends on the hardware used to realize it, which in turn depends on the scale of the problem. More complex algorithms must be realized via a microprocessor or programmable controller, and for problems in which transduction power is low, such implementations may demand static power consumption levels comparable with transduction power levels. In such applications, it is therefore useful to simplify feedback algorithms to decision processes that can be realized using simple analog networks, containing as few active components as possible. This observation leads to an interesting connection between stochastic energy harvesting problems, and fixed-structure and static control synthesis concepts.

Motivated by the above observation, the primary contributions of this paper are twofold. First, for the case where the electronics are capable of two-way power flow, we build upon the results presented in [12] to show that for stochastic disturbances characterized by second-order, bandpass-filtered white noise, energy harvesters can be passively "tuned" such that optimal stationary power generation only requires half of the system states for feedback in the active circuit. Interestingly, these states may often be the ones most easy to sense. For example, for a base-excited SDOF electromagnetic harvester, only the disturbance acceleration and transducer voltage are needed for feedback. The second contribution is the development of a sub-optimal, nonlinear controller for the case where the electronics are capable of only power extraction. Again, we show that tuning techniques can be used to retain the property that only half the states are required for feedback in the nonlinear controller. Power generation resulting from using both the unconstrained and constrained controllers is compared to the case where the electronic drive is controlled to create a purely resistive input impedance, and is then optimized for maximal absorption.

DISTURBANCE AND HARVESTER MODELS

For this discussion, we consider the case in which the disturbance acceleration $a(t)$ is modeled as filtered noise. We will assume that $a(t)$ has a power spectral density equal to

$$\Phi_a(\omega) = \left| \frac{qj\omega}{-\omega^2 + 2\omega_a\zeta_a j\omega + \omega_a^2} \right|^2 \tag{1}$$

where ω_a is the center of the passband of $a(t)$, and ζ_a determines the spread of its frequency content. For such a process, it is straight-forward to represent the disturbance dynamics by a two-dimensional state space of the form

$$\frac{d}{dt}\mathbf{x}_a(t) = \mathbf{A}_a\mathbf{x}_a(t) + \mathbf{B}_a w(t) \tag{2a}$$
$$a(t) = \mathbf{C}_a\mathbf{x}_a(t) \tag{2b}$$

where $w(t)$ is a white noise process with spectral intensity equal to unity. The parameter q in Equation (1) is adjusted such that irrespective of ω_a and ζ_a, $a(t)$ has a consistent standard deviation of σ_a; i.e.,

$$\sigma_a = \sqrt{\frac{1}{2\pi}\int_{-\infty}^{\infty} \Phi_a(\omega)d\omega}\,. \tag{3}$$

This allows us to compare disturbances of varying spectral content, but equal intensity. We refer to the "narrowband limit" for the disturbance model as the case in which $\zeta_a \to 0$. Similarly, refer to "broadband limit" as the case in which $\zeta_a \to \infty$.

We assume the harvester is a dissipative system and that the harvester dynamics can be approximated by a finite-dimensional linear state space. Let $H_a(s)$ and $H_i(s)$ be the transfer functions from the disturbance acceleration $a(t)$ and the control current $i(t)$, respectively, to the voltage generated by the system $v(t)$. We will assume both $H_a(s)$ and $H_i(s)$ to be strictly proper and that $H_i(s)$ is weakly strictly positive real (WSPR) [13]. With these assumptions, there always exists a self-dual state space realization [14] for the harvester, of the form

$$\frac{d}{dt}\mathbf{x}_h(t) = \mathbf{A}_h\mathbf{x}_h(t) + \mathbf{B}_h i(t) + \mathbf{G}_h a(t) \tag{4a}$$
$$v(t) = \mathbf{B}_h^T\mathbf{x}_h(t) \tag{4b}$$

This representation implies that $H_i(s) = \mathbf{B}_i^T(s\mathbf{I} - \mathbf{A}_h)^{-1}\mathbf{B}_i$ and $H_a(s) = \mathbf{B}_i^T(s\mathbf{I} - \mathbf{A}_h)^{-1}\mathbf{B}_a$. In the above realization, the total dissipation in the harvester at time t is $-\frac{1}{2}\mathbf{x}_h^T(t)[\mathbf{A}_h + \mathbf{A}_h^T]\mathbf{x}_h(t) \geqslant 0$, and the total energy stored in the harvester is $\frac{1}{2}\mathbf{x}_h^T(t)\mathbf{x}_h(t)$. The WSPR assumption allows us to assume that the pair $(\mathbf{A}_h, \mathbf{A}_h + \mathbf{A}_h^T)$ is observable, which implies that no response of the harvester can exhibit zero internal dissipation over any finite interval.

Combining the disturbance and harvester dynamics into an augmented state space yields

$$\frac{d}{dt}\mathbf{x}(t) = \mathbf{A}\mathbf{x}(t) + \mathbf{B}i(t) + \mathbf{G}w(t) \tag{5a}$$
$$v(t) = \mathbf{B}^T\mathbf{x}(t) \tag{5b}$$

where the augmented matrices $\mathbf{A}$, $\mathbf{B}$, and $\mathbf{G}$ are

$$\mathbf{A} = \begin{bmatrix} \mathbf{A}_h & \mathbf{G}_h\mathbf{C}_a \\ \mathbf{0} & \mathbf{A}_a \end{bmatrix}, \qquad \mathbf{B} = \begin{bmatrix} \mathbf{B}_h \\ \mathbf{0} \end{bmatrix}, \qquad \mathbf{G} = \begin{bmatrix} \mathbf{0} \\ \mathbf{B}_a \end{bmatrix} \tag{6}$$

and the resultant augmented state vector is

$$\mathbf{x}(t) = \left[\mathbf{x}_h^T(t)\ \mathbf{x}_a^T(t)\right]^T. \tag{7}$$

We make the assumption that $(\mathbf{A}, \mathbf{B}^T)$ is observable and $(\mathbf{A}, [\mathbf{B}\ \mathbf{G}])$ is controllable. If this is not the case for the original system model, we assume that dimension of the augmented state space has been reduced to a minimal realization.

EXAMPLES

We now introduce two example systems that will be the focus of the analysis for the remaining sections. The first involves electromagnetic transduction, while the second involves piezoelectric transduction. These two systems are shown in Figure 2.

Electromagnetic example

Consider the single-degree-of-freedom (SDOF) resonant oscillator with mass m, damping b, and stiffness k in Figure 2 (a). A transducer is attached between the base and the moving mass such that $f_e(t) = c_e i(t)$ where c_e is the coupling coefficient. This system corresponds to an energy harvester with electromagnetic coupling. Similar electromagnetic energy harvesting systems have been demonstrated in [15, 16]. The gov-

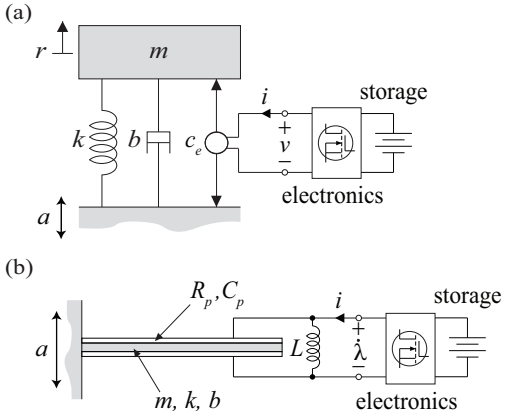

FIGURE 2. Passive energy harvesting systems: (a) SDOF oscillator with an electromagnetic actuator; (b) piezoelectric bimorph cantilever beam with an inductor connected in parallel.

erning equations for this system are

$$m\ddot{r}(t) + b\dot{r}(t) + kr(t) = ma(t) + c_e i(t) \tag{8a}$$
$$v(t) = c_e \dot{r}(t) \tag{8b}$$

where $r(t)$ is the displacement of the harvester. The corresponding power spectral density for the disturbance acceleration $a(t)$ is defined in Equation (1). If we make the following substitutions for time and displacement, respectively,

$$t = \sqrt{\frac{m}{k}}\,\tau, \qquad r(t) = \left(\frac{m\sigma_a}{k}\right)\bar{r}(\tau) \tag{9}$$

then the harvester dynamics can be expressed in nondimensional coordinates; i.e.,

$$\bar{\ddot{r}}(\tau) + d\bar{\dot{r}}(\tau) + \bar{r}(\tau) = \bar{a}(\tau) + \bar{i}(\tau) \tag{10a}$$
$$\bar{v}(\tau) = \bar{\dot{r}}(\tau) \tag{10b}$$

where the mechanical damping is

$$d = \frac{b}{\sqrt{mk}}\,. \tag{11}$$

It follows that the nondimensional acceleration, current, and voltage are, respectively,

$$a(t) = \sigma_a \bar{a}(\tau), \quad i(t) = \left(\frac{m\sigma_a}{c_e}\right)\bar{i}(\tau), \quad v(t) = \left(c_e\sigma_a\sqrt{\frac{m}{k}}\right)\bar{v}(\tau)\,. \tag{12}$$

The nondimensionalized harvester dynamics can be modeled by a two-dimensional state vector $\mathbf{x}_h(\tau) = \left[\bar{r}(\tau)\ \bar{\dot{r}}(\tau)\right]^T$ such that

$$\mathbf{A}_h = \begin{bmatrix} 0 & 1 \\ -1 & -d \end{bmatrix}, \qquad \mathbf{B}_h = \begin{bmatrix} 0 \\ 1 \end{bmatrix}, \qquad \mathbf{G}_h = \begin{bmatrix} 0 \\ 1 \end{bmatrix}. \tag{13}$$

We assume that the harvester has been tuned such that its natural frequency is in the center of the disturbance passband. This implies that the power spectrum of $\bar{a}(\tau)$ can be expressed (in normalized frequency $\bar{\omega} = \omega\sqrt{m/k}$) as

$$\Phi_{\bar{a}}(\bar{\omega}) = \left|\frac{\bar{q}\,j\bar{\omega}}{-\bar{\omega}^2 + 2\zeta_a j\bar{\omega} + 1}\right|^2 \tag{14}$$

with $\bar{q}$ chosen such that $\int_{-\infty}^{\infty}\Phi_{\bar{a}}(\bar{\omega})\,d\bar{\omega} = 1$. It turns out that the value of $\bar{q}$ which brings this about is $\bar{q} = 2\sqrt{\zeta_a}$. Thus, the nondimensionalized disturbance dynamics can be modeled by a two-dimensional state vector $\mathbf{x}_a(\tau) = \left[\int\bar{a}(\tau)\ \bar{a}(\tau)\right]^T$ such that

$$\mathbf{A}_a = \begin{bmatrix} 0 & 1 \\ -1 & -2\zeta_a \end{bmatrix}, \quad \mathbf{B}_a = \begin{bmatrix} 0 \\ 2\sqrt{\zeta_a} \end{bmatrix}, \quad \mathbf{C}_a = \begin{bmatrix} 0 \\ 1 \end{bmatrix}^T. \tag{15}$$

Combining the harvester and disturbance models into an equivalent augmented form results in the following representation for the dynamics and input matrices

$$\mathbf{A} = \begin{bmatrix} 0 & 1 & 0 & 0 \\ -1 & -d & 0 & 1 \\ 0 & 0 & 0 & 1 \\ 0 & 0 & -1 & -2\zeta_a \end{bmatrix}, \quad \mathbf{B} = \begin{bmatrix} 0 \\ 1 \\ 0 \\ 0 \end{bmatrix}, \quad \mathbf{G} = \begin{bmatrix} 0 \\ 0 \\ 0 \\ 2\sqrt{\zeta_a} \end{bmatrix}. \tag{16}$$

Piezoelectric example

Consider the piezoelectric bimorph cantilever beam in Figure 2 (b). The transducer has an equivalent capacitance C_p and dielectric leakage resistance R_p. We assume that the deflection at the end of the cantilever beam can be modeled by a finite summation of Galerkin mode shapes. As such, the differential equations describing the dynamics of the beam can be approximated through a standard Rayleigh-Ritz projection. Keeping only the fundamental vibratory mode, we approximate the beam by a mass m, a stiffness k, and a coupling coefficient θ. In addition, a Rayleigh damping term b is assumed for the beam. As seen in Figure 2 (b) the terminals of the piezoelectric patch are connected in parallel to an inductor with inductance L. Given the assumptions about the dynamics of the beam, the governing equations for this system are

$$m\ddot{r}(t) + b\dot{r}(t) + kr(t) = \Gamma a(t) - \theta\dot{\lambda}(t) \tag{17a}$$
$$C_p\ddot{\lambda}(t) + \frac{1}{R_p}\dot{\lambda}(t) + \frac{1}{L}\lambda(t) = i(t) + \theta\dot{r}(t) \tag{17b}$$

where $\lambda(t)$ is the flux linkage across the piezoelectric patch, $r(t)$ is the displacement of the beam, and Γ is an equivalent mass term.

Next, if we make the following substitutions for time, displacement, and flux, respectively,

$$t = \sqrt{\frac{m}{k}}\,\tau, \quad r(t) = \left(\frac{m\sigma_a}{k}\right)\bar{r}(\tau), \quad \lambda(t) = \left(\frac{m\sigma_a}{k}\sqrt{\frac{m}{C_p}}\right)\bar{\lambda}(\tau) \tag{18}$$

then the system can be expressed in nondimensional coordinates; i.e.,

$$\bar{\ddot{r}}(\tau) + d\bar{\dot{r}}(\tau) + \bar{r}(\tau) = \bar{a}(\tau) - \bar{\dot{\lambda}}(\tau) \tag{19a}$$
$$\bar{\ddot{\lambda}}(\tau) + \beta\bar{\dot{\lambda}}(\tau) + \alpha\bar{\lambda}(\tau) = \bar{i}(\tau) + \bar{\dot{r}}(\tau)\,. \tag{19b}$$

The nondimensional mechanical damping of the beam d remains unchanged from the previous example and the electrical damping is

$$\beta = \frac{1}{C_p R_p}\sqrt{\frac{m}{k}}\,. \tag{20}$$

It follows that the remaining nondimensional parameters are

$$a(t) = \left(\frac{m\sigma_a}{\Gamma}\right)\bar{a}(\tau), \quad i(t) = \left(\theta\sigma_a\sqrt{\frac{m}{k}}\right)\bar{i}(\tau), \quad \alpha = \frac{m}{kC_pL}\,. \tag{21}$$

We assume that the state space describing the disturbance dynamics is the same as the state space defined in the previous example. Thus, we have that the augmented state space characterizing the piezoelectric harvester and disturbance dynamics can be expressed as

$$\mathbf{A} = \begin{bmatrix} \mathbf{0} & \mathbf{I} & \mathbf{0} & \mathbf{0} \\ -\mathbf{S} & -\mathbf{D} & \mathbf{0} & \mathbf{B}_2 \\ \mathbf{0} & \mathbf{0} & 0 & 1 \\ \mathbf{0} & \mathbf{0} & -1 & -2\zeta_a \end{bmatrix}, \quad \mathbf{B} = \begin{bmatrix} \mathbf{0} \\ \mathbf{B}_1 \\ 0 \\ 0 \end{bmatrix}, \quad \mathbf{G} = \begin{bmatrix} \mathbf{0} \\ \mathbf{0} \\ 0 \\ 2\sqrt{\zeta_a} \end{bmatrix} \tag{22}$$

where

$$\mathbf{D} = \begin{bmatrix} d & 1 \\ -1 & \beta \end{bmatrix}, \quad \mathbf{S} = \begin{bmatrix} 1 & 0 \\ 0 & \alpha \end{bmatrix}, \quad \mathbf{B}_1 = \begin{bmatrix} 0 \\ 1 \end{bmatrix}, \quad \mathbf{B}_2 = \begin{bmatrix} 1 \\ 0 \end{bmatrix}\,. \tag{23}$$

It should be noted that the harvester dynamics are modeled by a four-dimensional state vector $\mathbf{x}_h(\tau) = \left[\bar{r}(\tau)\ \bar{\lambda}(\tau)\ \dot{\bar{r}}(\tau)\ \dot{\bar{\lambda}}(\tau)\right]^T$.

We will henceforth uniformly assume that the electromagnetic example and the piezoelectric example have been nondimensionalized by Equation (10) and Equation (19), respectively. To ease the notation, we will do away with all overbars and refer to the nondimensional time as t.

OPTIMAL STATIC ENERGY HARVESTING

One of the simplest ways to absorb power in an energy harvesting system is by controlling the electronics to emulate a resistive load. For the case where the disturbance is stochastic, this can be accomplished by having the electronics simulate a static admittance across the terminals of the transducer, and then tune this admittance to maximize the average power generated. To optimize the static admittance, first we define the power delivered to storage as the power extracted by the transducer, minus the transmission losses in the power electronic circuitry. If we approximate these losses as resistive, with some resistance R, then the power delivered to storage is

$$P_s(t) = -i(t)v(t) - Ri^2(t)\,. \tag{24}$$

The objective is to maximize the expectation of the power delivered to storage by determining the optimal static admittance.

By convention, when the electronics are implementing a static admittance the current input is $i(t) = -Y_c v(t)$. Substituting this relationship into Equation (5), results in the augmented closed-loop dynamics having the form

$$\tfrac{d}{dt}\mathbf{x}(t) = \left[\mathbf{A} - \mathbf{B}Y_c\mathbf{B}^T\right]\mathbf{x}(t) + \mathbf{G}w(t)\,. \tag{25}$$

The stationary covariance matrix $\mathbf{\Sigma} = \mathscr{E}\{\mathbf{x}(t)\mathbf{x}^T(t)\}$ is found by solving the Lyapunov equation

$$\left[\mathbf{A} - \mathbf{B}Y_c\mathbf{B}^T\right]\mathbf{\Sigma} + \mathbf{\Sigma}\left[\mathbf{A} - \mathbf{B}Y_c\mathbf{B}^T\right]^T + \mathbf{G}\mathbf{G}^T = \mathbf{0} \tag{26}$$

and the resultant average power generation is the expectation of Equation (24); i.e.,

$$\bar{P}_{gen} = \left(Y_c - Y_c^2 R\right)\mathbf{B}^T\mathbf{\Sigma}\mathbf{B}\,. \tag{27}$$

Because the system only has one design parameter (i.e., Y_c) in this case, the most straight-forward way to optimize $\bar{P}_{gen}$ is via a one-dimensional line search. One can, for example, employ the bisection algorithm to converge rapidly to the optimal Y_c, given $\mathbf{A}$, $\mathbf{B}$, $\mathbf{G}$, and R.

OPTIMAL, UNCONSTRAINED ENERGY HARVESTING

For the case where the electronics are capable of two-way power flow, we presume that the the entire system state $\mathbf{x}(t)$ is available for feedback. In this case, the design problem involves the design of a causal feedback law $\mathbf{x} \mapsto i$. The objective is to find the particular feedback law which maximizes the average power generated in stationary stochastic response. If we take the expectation of both sides of Equation (24), then we can define the average power generated as the expectation of the power delivered to storage; i.e.,

$$\bar{P}_{gen} = -\mathscr{E}\{i(t)\mathbf{B}^T\mathbf{x}(t) + Ri^2(t)\}\,. \tag{28}$$

This is equivalent to a LQG optimal control problem. We define the cost function as

$$J = \mathscr{E}\left\{\begin{bmatrix}\mathbf{x}(t)\\ i(t)\end{bmatrix}^T\begin{bmatrix}\mathbf{0} & \frac{1}{2}\mathbf{B}\\ \frac{1}{2}\mathbf{B}^T & R\end{bmatrix}\begin{bmatrix}\mathbf{x}(t)\\ i(t)\end{bmatrix}\right\}. \tag{29}$$

Minimizing the cost function J is equivalent to maximizing $\bar{P}_{gen}$.

Theorem 1. *Over the space of all causal, continuous feedback functions, the optimal energy harvesting current is characterized by the linear state feedback relationship*

$$i(t) = \mathbf{K}\mathbf{x}(t) \tag{30}$$

where

$$\mathbf{K} = -\frac{1}{R}\mathbf{B}^T\left(\mathbf{P}+\tfrac{1}{2}\mathbf{I}\right) \tag{31}$$

and $\mathbf{P} = \mathbf{P}^T < 0$ *is the unique, stabilizing solution to the non-standard Riccati equation*

$$\mathbf{A}^T\mathbf{P} + \mathbf{P}\mathbf{A} - \frac{1}{R}\left(\mathbf{P}+\tfrac{1}{2}\mathbf{I}\right)\mathbf{B}\mathbf{B}^T\left(\mathbf{P}+\tfrac{1}{2}\mathbf{I}\right) = \mathbf{0}\,. \tag{32}$$

The optimal average power generated is

$$\bar{P}_{gen} = -\mathbf{G}^T\mathbf{P}\mathbf{G}\,. \tag{33}$$

Proof. A proof of this theorem can be found in [7].

Implementing the state feedback control law in Equation (30) generally requires knowledge of every state in the system. In other words, every component in the feedback gain matrix $\mathbf{K}$ will in general be nonzero. However, it turns out that if the augmented system can be expressed in the realization described in the Section "Disturbance and Harvester Models", then the stabilizing solution $\mathbf{P}$ to the Riccati equation in Equation (32) has a special structure. Specifically, $\mathbf{P}$ has several block entries that are equal to zero and several non-zero block entries that are repeated. As a result of this, the solution for $\mathbf{K}$ in Equation (31) then has many entries which are also zero. We now present a theorem which formally introduces these concepts.

Theorem 2. *If the harvester dynamics can be expressed as*

$$\mathbf{A}_h = \begin{bmatrix}\mathbf{0} & \mathbf{I}\\ -\mathbf{I} & -\mathbf{D}\end{bmatrix}, \qquad \mathbf{B}_h = \begin{bmatrix}\mathbf{0}\\ \mathbf{B}_1\end{bmatrix}, \qquad \mathbf{G}_h = \begin{bmatrix}\mathbf{0}\\ \mathbf{B}_2\end{bmatrix} \tag{34}$$

and the disturbance dynamics can be expressed as

$$\mathbf{A}_a = \begin{bmatrix}\mathbf{0} & \mathbf{I}\\ -\mathbf{I} & -\mathbf{Z}\end{bmatrix}, \qquad \mathbf{B}_a = \begin{bmatrix}\mathbf{0}\\ \mathbf{Q}\end{bmatrix}, \qquad \mathbf{C}_a = \begin{bmatrix}\mathbf{0}\\ \mathbf{I}\end{bmatrix}^T \tag{35}$$

then the unique, stabilizing solution to the Riccati equation in Equation (32) *is*

$$\mathbf{P} = \begin{bmatrix}\mathbf{P}_{22} & \mathbf{0} & \mathbf{P}_{24} & \mathbf{0}\\ \mathbf{0} & \mathbf{P}_{22} & \mathbf{0} & \mathbf{P}_{24}\\ \mathbf{P}_{24}^T & \mathbf{0} & \mathbf{P}_{44} & \mathbf{0}\\ \mathbf{0} & \mathbf{P}_{24}^T & \mathbf{0} & \mathbf{P}_{44}\end{bmatrix} \tag{36}$$

where $\mathbf{P}_{22}$, $\mathbf{P}_{24}$, *and* $\mathbf{P}_{44}$ *can be solved sequentially as*

$$\mathbf{P}_{22}\mathbf{D} + \mathbf{D}^T\mathbf{P}_{22} + \frac{1}{R}\left(\mathbf{P}_{22}+\tfrac{1}{2}\mathbf{I}\right)\mathbf{B}_1\mathbf{B}_1^T\left(\mathbf{P}_{22}+\tfrac{1}{2}\mathbf{I}\right) = \mathbf{0}\,, \tag{37}$$

$$\mathbf{P}_{22}\mathbf{B}_2 - \mathbf{P}_{24}\mathbf{Z} - \mathbf{D}^T\mathbf{P}_{24} - \frac{1}{R}\left(\mathbf{P}_{22}+\tfrac{1}{2}\mathbf{I}\right)\mathbf{B}_1\mathbf{B}_1^T\mathbf{P}_{24} = \mathbf{0}\,, \tag{38}$$

$$\mathbf{P}_{24}^T\mathbf{B}_2 + \mathbf{B}_2^T\mathbf{P}_{24} - \mathbf{P}_{44}\mathbf{Z} - \mathbf{Z}^T\mathbf{P}_{44} - \frac{1}{R}\mathbf{P}_{24}^T\mathbf{B}_1\mathbf{B}_1^T\mathbf{P}_{24} = \mathbf{0}\,. \tag{39}$$

For the state vector partitioned analogously to $\mathbf{P}$*, the corresponding optimal gain matrix is*

$$\mathbf{K} = \begin{bmatrix}\mathbf{0} & -\frac{1}{R}\mathbf{B}_1\left(\mathbf{P}_{22}+\frac{1}{2}\mathbf{I}\right) & \mathbf{0} & -\frac{1}{R}\mathbf{B}_1\mathbf{P}_{24}\end{bmatrix} \tag{40}$$

and the optimal power generation is

$$\bar{P}_{gen} = -\mathbf{Q}^T\mathbf{P}_{44}\mathbf{Q} \tag{41}$$

Proof. A proof of this theorem can be found in [17].

From this theorem, we obtain the interesting result that only half of the states are required for the optimal energy harvesting current.

Electromagnetic example

Returning to the electromagnetic energy harvesting example, it is clear that the matrices in Equation (16) satisfy the conditions in Theorem 2. As such, the corresponding decoupled solution to the Riccati equation is

$$\mathbf{P} = \begin{bmatrix}P_{22} & 0 & P_{24} & 0\\ 0 & P_{22} & 0 & P_{24}\\ P_{24} & 0 & P_{44} & 0\\ 0 & P_{24} & 0 & P_{44}\end{bmatrix}. \tag{42}$$

Next, we can solve for P_{22}, P_{24}, and P_{44} by sequentially solving Equations (37), (38), and (39); i.e.,

$$2dP_{22} + \frac{1}{R}(P_{22}+\tfrac{1}{2})(P_{22}+\tfrac{1}{2}) = 0\,, \tag{43}$$

$$P_{22} - P_{24}(2\zeta_a + d) - \frac{1}{R}(P_{22}+\tfrac{1}{2})P_{24} = 0\,, \tag{44}$$

$$2P_{24} - 4\zeta_a P_{44} - \frac{1}{R}P_{24}^2 = 0\,. \tag{45}$$

In this case it is possible to find the closed form, negative definite solution to Equation (42). From this solution, we can solve for the symbolic solution for the optimal energy harvesting current as

$$i(t) = K_v v(t) + K_a a(t)\,. \tag{46}$$

Furthermore, we can solve for the symbolic solution for the corresponding optimal harvested power. Since the derivation of the optimal gains and harvested power is quite lengthy, we refer interested readers to [17].

Piezoelectric example

Next, we return to the piezoelectric energy harvesting example. The augmented harvester and disturbance model in Equation (22) satisfies the conditions in Theorem 2 if $\mathbf{S} = \mathbf{I}$, which can be accomplished by setting $\alpha = 1$. Upon closer inspection of α, we see that it is the square of the reciprocal of the natural frequency of the equivalent electrical dynamics multiplied by the first natural frequency of the cantilever beam. As such, for a typical piezoelectric energy harvesting system, an extremely large inductor would typically be required for α to equal unity. However, for the purpose of this example, we assume that the value of α is unconstrained and can be tuned via the inductance value L. It turns out that tuning a passive network containing an inductor and a resistor in parallel is exactly what one would do to impedance-match a piezoelectric energy harvester for resonant performance [10]. If we set $\alpha = 1$ then we have that the dynamics matrix is

$$\mathbf{A} = \begin{bmatrix} \mathbf{0} & \mathbf{I} & \mathbf{0} & \mathbf{0} \\ -\mathbf{I} & -\mathbf{D} & \mathbf{0} & \mathbf{B}_2 \\ \mathbf{0} & \mathbf{0} & 0 & 1 \\ \mathbf{0} & \mathbf{0} & -1 & -2\zeta_a \end{bmatrix} \tag{47}$$

and the corresponding decoupled solution to the Riccati equation is

$$\mathbf{P} = \begin{bmatrix} \mathbf{P}_{22} & \mathbf{0} & \mathbf{P}_{24} & \mathbf{0} \\ \mathbf{0} & \mathbf{P}_{22} & \mathbf{0} & \mathbf{P}_{24} \\ \mathbf{P}_{24}^T & \mathbf{0} & P_{44} & 0 \\ \mathbf{0} & \mathbf{P}_{24}^T & 0 & P_{44} \end{bmatrix} . \tag{48}$$

We can solve for $\mathbf{P}_{22}$, $\mathbf{P}_{24}$, and P_{44} by sequentially solving Equations (37), (38), and (39); i.e.,

$$\mathbf{P}_{22}\mathbf{D} + \mathbf{D}^T\mathbf{P}_{22} + \frac{1}{R}\left(\mathbf{P}_{22} + \tfrac{1}{2}\mathbf{I}\right)\mathbf{B}_1\mathbf{B}_1^T\left(\mathbf{P}_{22} + \tfrac{1}{2}\mathbf{I}\right) = \mathbf{0} , \tag{49}$$

$$\mathbf{P}_{22}\mathbf{B}_2 - 2\zeta_a\mathbf{P}_{24} - \mathbf{D}^T\mathbf{P}_{24} - \frac{1}{R}\left(\mathbf{P}_{22} + \tfrac{1}{2}\mathbf{I}\right)\mathbf{B}_1\mathbf{B}_1^T\mathbf{P}_{24} = \mathbf{0} , \tag{50}$$

$$\mathbf{P}_{24}^T\mathbf{B}_2 + \mathbf{B}_2^T\mathbf{P}_{24} - 4\zeta_a P_{44} - \frac{1}{R}\mathbf{P}_{24}^T\mathbf{B}_1\mathbf{B}_1^T\mathbf{P}_{24} = \mathbf{0} . \tag{51}$$

For this example it is not possible to find a closed form solution for $\mathbf{P}$. This is due to the fact that Equation (49) is a Riccati equation and $\mathbf{D}$ is a full 2×2 matrix. However, once a numerical solution for $\mathbf{P}_{22}$ has been determined, we can easily solve for $\mathbf{P}_{24}$ and P_{44}. From Theorem 2, we note that only the mechanical velocity $\dot{r}(t)$, the piezoelectric voltage $\dot{\lambda}(t)$, and the disturbance acceleration $a(t)$ are required to enforce the optimal current input. As such, the optimal control law for the piezoelectric energy harvester is

$$i(t) = K_{\dot{r}}\dot{r}(t) + K_v v(t) + K_a a(t) \tag{52}$$

where $K_{\dot{r}}$ is the mechanical velocity gain and $v(t) = \dot{\lambda}(t)$.

The optimal feedback control laws in Equations (46) and (52) are realized by summing static gains of measured system states. For both systems, the states required for feedback are the easiest to sense. It may therefore be straightforward in many applications to design an analog circuit to realize the optimal control law and an example circuit is presented in [17].

SUB-OPTIMAL, POWER-FLOW CONSTRAINED ENERGY HARVESTING

For the case where the electronics are limited to power extraction, we now present an analytically-tractable manner by which we can achieve performance which is better than that with the electronics implementing the optimal static admittance. The effective input resistance of the buck-boost converter in Figure 1 (a) has a value which is proportional to the inverse-square of the duty cycle D of its MOSFET; i.e.,

$$R_c(t) = R_{c0} + R_{c1}D^{-2} . \tag{53}$$

The duty cycle value can range on the open interval from $(0, D_{max})$, where D_{max} is the duty cycle at which the converter transitions from the discontinuous to continuous conduction regime. As such, an advantage of this approach is that one can adjust the effective resistance of the power electronics by adjusting D, and the resultant electromechanical dynamics of the harvester can be approximated as equivalent to those with the electronics replaced by a time-varying resistive shunt. It also means that one can optimize the power extraction for the system by optimizing a time-varying admittance (i.e., $Y_c(t) = 1/R_c(t)$), over the range

$$Y_c(t) \in [Y_c^{min}, Y_c^{max}] = \left[0, \frac{D_{max}^2}{R_{c0}D_{max}^2 + R_{c1}}\right] . \tag{54}$$

Given these assumptions, we have that the constraint on power flow that the electronics must satisfy is

$$i(t)v(t) + i^2(t)/Y_c^{max} \leqslant 0, \ \ \forall t . \tag{55}$$

Let the optimal static value of Y_c, be denoted $Y_c^* \in (0, Y_c^{max})$. Also, let the corresponding value of $\mathbf{\Sigma}$, resulting from Equation (26) with $Y_c(t) = Y_c^*$, be denoted $\mathbf{\Sigma}^*$. Then we have that the performance with $Y_c(t) = Y_c^*$, $\forall t$, is $\tilde{P}_{gen}\big|_{Y_c(t)=Y_c^*} = (Y_c^* - Y_c^{*2}R)\mathbf{B}^T\mathbf{\Sigma}^*\mathbf{B}$. Now, we note an important theorem from nonlinear stochastic control.

Theorem 3. *Let $i(t) = \phi(\mathbf{x}(t))$ be any continuous stabilizing nonlinear feedback law. Then with this feedback law imposed on a general state space system characterized by Equation* (5)*, the average power generation is*

$$\bar{P}_{gen} = (Y_c^* - Y_c^{*2}R)\mathbf{B}^T\mathbf{\Sigma}^*\mathbf{B} + R\mathscr{E}\left\{-\left(i(t) - \hat{\mathbf{K}}\mathbf{x}(t)\right)^2 + \left(Y_c^* v(t) + \hat{\mathbf{K}}\mathbf{x}(t)\right)^2\right\} \tag{56}$$

where

$$\hat{\mathbf{K}} = -\tfrac{1}{R}\mathbf{B}^T\left(\hat{\mathbf{P}} + \tfrac{1}{2}\mathbf{I}\right) \tag{57}$$

and $\hat{\mathbf{P}}$ *is the unique solution to the Lyapunov equation*

$$\left[\mathbf{A} - \mathbf{B}Y_c^*\mathbf{B}^T\right]^T\hat{\mathbf{P}} + \hat{\mathbf{P}}\left[\mathbf{A} - \mathbf{B}Y_c^*\mathbf{B}^T\right] + \mathbf{B}\left(-Y_c^* + Y_c^{*2}R\right)\mathbf{B}^T = 0\,. \tag{58}$$

Proof. A proof of this theorem can be found in [18].

In the above theorem we see that the expression for $\bar{P}_{gen}$ in Equation (56) is a summation of two terms. The first of these is actually the value of $\bar{P}_{gen}$ if $Y_c(t) = Y_c^*$, $\forall t$. The second term (i.e., the expectation) does not in general have a closed form unless ϕ is linear. However, we know that for any $\mathbf{x}(t)$, there always exists at least one corresponding $i(t)$ which makes the argument in the expectation negative, because for every time, $i(t) = -Y_c^* v(t)$ is guaranteed to satisfy feasibility criterion in Equation (55). It is therefore a provable fact that the nonlinear relationship characterized by the simple saturation

$$i(t) = \underset{iv+i^2/Y_c^{max}\leqslant 0}{\operatorname{argmin}} \left\{i(t) - \hat{\mathbf{K}}\mathbf{x}(t)\right\}^2 \tag{59}$$

$$= \underset{iv+i^2/Y_c^{max}\leqslant 0}{\operatorname{sat}} \left\{\hat{\mathbf{K}}\mathbf{x}(t)\right\} \tag{60}$$

will guarantee to increase $\bar{P}_{gen}$ beyond the case with $Y_c(t) = Y_c^*$, $\forall t$. The function $\operatorname{sat}(\cdot)$ is the saturation function, which restricts $i(t)$ to the power flow constraint. Note that this observation is actually true for all harvester models adhering to Equation (5).

Electromagnetic example

For the electromagnetic energy harvester, we have the same convenient decoupling conditions for the constrained controller as we did with the unconstrained controller. It turns out that in this case $\hat{\mathbf{P}}$ has the same special structure as in the unconstrained case, i.e., Equation (42), with $\hat{P}_{22}$, $\hat{P}_{24}$, and $\hat{P}_{44}$ defined as

$$\hat{P}_{22} = \frac{-Y_c^* + Y_c^{*2}R}{2\left(d + Y_c^*\right)}\,, \tag{61}$$

$$\hat{P}_{24} = \frac{-Y_c^* + Y_c^{*2}R}{2\left(d + Y_c^*\right)\left(d + Y_c^* + 2\zeta_a\right)}\,, \tag{62}$$

$$\hat{P}_{44} = \frac{-Y_c^* + Y_c^{*2}R}{4\zeta_a\left(d + Y_c^*\right)\left(d + Y_c^* + 2\zeta_a\right)}\,. \tag{63}$$

Consequently, we can express the feedback relationship in Equation (60) with the decoupled gain matrix in Equation (40) as

$$i(t) = -\underset{iv+i^2/Y_c^{max}\leqslant 0}{\operatorname{sat}} \left\{\hat{K}_v v(t) + \hat{K}_a a(t)\right\} \tag{64}$$

where

$$\hat{K}_v = \frac{-Y_c^* + Y_c^{*2}R}{2R\left(d + Y_c^*\right)} + \frac{1}{2R}\,, \tag{65}$$

$$\hat{K}_a = \frac{-Y_c^* + Y_c^{*2}R}{2R\left(d + Y_c^*\right)\left(d + Y_c^* + 2\zeta_a\right)}\,. \tag{66}$$

Recognizing that $i(t) = -Y_c(t)v(t)$, this implies an equation to determine the time-varying $Y_c(t)$ for this controller directly, as

$$Y_c(t) = \underset{[0,Y_c^{max}]}{\operatorname{sat}} \left\{\hat{K}_v + \hat{K}_a\frac{a(t)}{v(t)}\right\}\,. \tag{67}$$

The argument in the brackets consists of a constant term, plus a term that varies with the ratio $a(t)/v(t)$. It is this variable term that is responsible for the improvement in performance over the constant Y_c^* case, for the electromagnetic energy harvester.

Piezoelectric example

If we set $\alpha = 1$ to satisfy the conditions in Theorem 2, then the expression for $\hat{\mathbf{P}}$ has the same structure as the unconstrained controller in Equation (48). However, unlike the unconstrained controller, we can find a closed form solution to $\hat{\mathbf{P}}$ for the piezoelectric energy harvester. In this case $\hat{\mathbf{P}}_{22}$, $\hat{\mathbf{P}}_{24}$, and $\hat{P}_{44}$ can be expressed as

$$\hat{\mathbf{P}}_{22} = \frac{-Y_c^* + Y_c^{*2}R}{2\gamma_1}\begin{bmatrix}1 & d\\ d & 1 + \beta d + d^2 + dY_c^*\end{bmatrix}, \tag{68}$$

$$\hat{\mathbf{P}}_{24} = \frac{-Y_c^* + Y_c^{*2}R}{2\gamma_1\gamma_2}\begin{bmatrix}\beta + d + Y_c^* + 2\zeta_a\\ d^2 + 2d\zeta_a - 1\end{bmatrix}, \tag{69}$$

$$\hat{P}_{44} = \frac{\left(-Y_c^* + Y_c^{*2}R\right)\left(\beta + d + Y_c^* + 2\zeta_a\right)}{4\zeta_a\gamma_1\gamma_2} \tag{70}$$

where

$$\gamma_1 = \beta + d + \beta^2 d + \beta d^2 + Y_c^* + 2\beta dY_c^* + d^2Y_c^* + dY_c^*\,, \tag{71}$$

$$\gamma_2 = 1 + \beta d + dY_c^* + 2\beta\zeta_a + 2d\zeta_a + 2\zeta_aY_c^* + 4\zeta_a^2\,. \tag{72}$$

If we define $\dot{\lambda}(t) = v(t)$, then we can express the feedback relationship in Equation (60) with the decoupled gain matrix in Equation (40) as

$$i(t) = -\underset{iv+i^2/Y_c^{max}\leqslant 0}{\operatorname{sat}} \left\{\hat{K}_{\dot{r}}\dot{r}(t) + \hat{K}_v v(t) + \hat{K}_a a(t)\right\} \tag{73}$$

where

$$\hat{K}_{\dot{r}} = \frac{d\left(-Y_c^* + Y_c^{*2}R\right)}{2R\gamma_1}\,, \tag{74}$$

$$\hat{K}_v = \frac{\left(1+\beta d+d^2+dY_c^*\right)\left(-Y_c^*+Y_c^{*2}R\right)}{2R\gamma_1}\,, \tag{75}$$

$$\hat{K}_a = \frac{\left(d^2+2d\zeta_a-1\right)\left(-Y_c^*+Y_c^{*2}R\right)}{2R\gamma_1\gamma_2}\,. \tag{76}$$

Again, recognizing that $i(t) = -Y_c(t)v(t)$, this implies an equation to determine the time-varying $Y_c(t)$ for this controller directly, as

$$Y_c(t) = \underset{[0,Y_c^{max}]}{\text{sat}}\left\{\hat{K}_v + \hat{K}_{\dot{r}}\frac{\dot{r}(t)}{v(t)} + \hat{K}_a\frac{a(t)}{v(t)}\right\}\,. \tag{77}$$

For the piezoelectric energy harvester, we have two variable terms that are responsible for the improvement in performance over the constant Y_c^* case.

SIMULATION EXAMPLES

To illustrate the potential for improvement in energy harvesting performace, we will present results in terms of a "$\bar{P}_{gen}$ ratio." The unconstrained $\bar{P}_{gen}$ ratio will be defined as the ratio of the average power generated with the electronics implementing the optimal static admittance over the average power generated with the electronics implementing the optimal unconstrained feedback control law (i.e., Equation (27) divided by Equation (41)). Similarly, the constrained $\bar{P}_{gen}$ ratio will be defined as the ratio of the average power generated with the electronics implementing the optimal static admittance over the average power generated with the electronics implementing the sub-optimal, power-flow constrained control law (i.e., Equation (27) divided by Equation (56)).

Unconstrained $\bar{P}_{gen}$ Ratio

First, we present results illustrating the unconstrained $\bar{P}_{gen}$ ratio for both the electromagnetic and piezoelectric energy harvesting examples. Figure 3 shows the unconstrained $\bar{P}_{gen}$ ratio for the electromagnetic energy harvester for various values of d and R, and for ranges of $\zeta_a \in [0,1]$. Similarly, Figure 4 shows the unconstrained $\bar{P}_{gen}$ ratio for the piezoelectric energy harvester for various values of d, β, and R, and for ranges of $\zeta_a \in [0,1]$. From these plots we see that there is a finite bandwidth for $a(t)$ at which knowledge of the derivative of the harvester states together with the disturbance acceleration is most beneficial. For the electromagnetic harvester, we see that knowledge of these states greatly improves performance over the entire range of ζ_a values for the asymptotic case where $R \to 0$. However, this is not true for the piezoelectric harvester as we see that the $\bar{P}_{gen}$ ratio appears to bend upwards after it reaches a minimal value.

Constrained $\bar{P}_{gen}$ Ratio

Next, we present results illustrating the constrained $\bar{P}_{gen}$ ratio for both the electromagnetic and piezoelectric energy harvesting examples. It should be noted that since Equation (56) does not have a closed-form solution, simulations of the dynamics of the energy harvesting systems implementing the nonlinear controller were conducted to determine an estimate of this value. It was found that 6000 seconds of simulation time at a sample rate of 100Hz provides an accurate estimate of Equation (56) for a given system. Figure 5 shows the constrained $\bar{P}_{gen}$ ratio

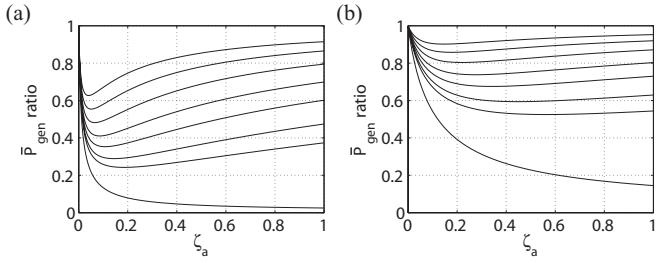

FIGURE 3. Unconstrained $\bar{P}_{gen}$ ratio for the electromagnetic energy harvester for R values of 0, 0.05, 0.08, 0.14, 0.22, 0.37, 0.61, 1 (from bottom to top): (a) $d = 0.01$; (b) $d = 0.1$.

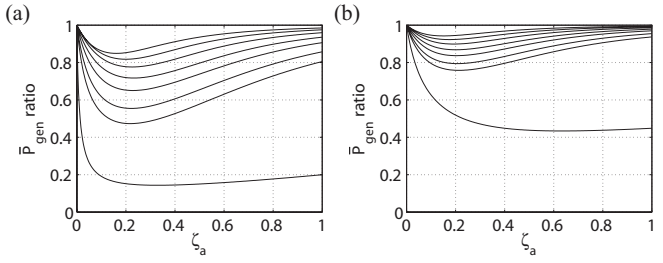

FIGURE 4. Unconstrained $\bar{P}_{gen}$ ratio for the piezoelectric energy harvester for R values of 0, 0.05, 0.08, 0.14, 0.22, 0.37, 0.61, 1 (from bottom to top): (a) $d = 0.01$ and $\beta = 0.01$; (b) $d = 0.1$ and $\beta = 0.01$.

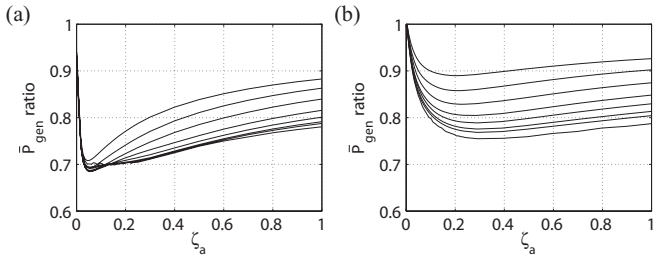

FIGURE 5. Constrained $\bar{P}_{gen}$ ratio for the electromagnetic energy harvester for R values of 0, 0.05, 0.08, 0.14, 0.22, 0.37, 0.61, 1 (from bottom to top): (a) $d = 0.01$; (b) $d = 0.1$.

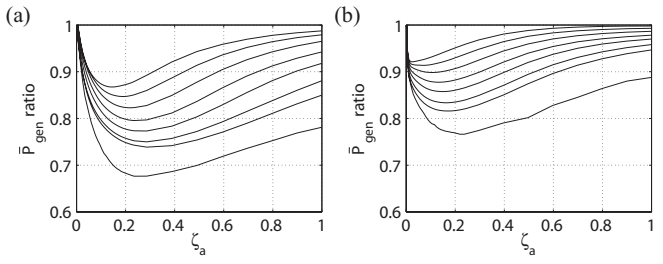

FIGURE 6. Constrained $\bar{P}_{gen}$ ratio for the piezoelectric energy harvester for R values of 0, 0.05, 0.08, 0.14, 0.22, 0.37, 0.61, 1 (from bottom to top): (a) $d = 0.01$ and $\beta = 0.01$; (b) $d = 0.1$ and $\beta = 0.01$.

for the electromagnetic energy harvester for various values of d and R, and for ranges of $\zeta_a \in [0,1]$. Similarly, Figure 6 shows the constrained $\bar{P}_{gen}$ ratio for the piezoelectric energy harvester for various values of d, β, and R, and for ranges of $\zeta_a \in [0,1]$. Again we note that both of these plots show that there is a finite bandwidth for $a(t)$ at which knowledge of the derivative of the harvester states together with the disturbance acceleration is most beneficial. We see that unconstrained controller improves the average power generated for all values of R and ζ_a, but that it is most effective for power electronics with low levels of parasitic losses.

CONCLUSIONS

The primary purpose of this paper has been to investigate the potential for enhanced energy harvesting performance from stochastic disturbances, through the use of feedback control laws that are specifically tailored for electronics with power-flow constraints. Firstly, for the case where power-flow is unconstrained, it turns out that the Riccati equation can be decoupled such that only the disturbance acceleration along with the derivative of the harvester states are needed for the optimal feedback control law. Secondly, for the case where power-flow is constrained to extration, we show that the average power generated using the optimal static admittance can be improved with a nonlinear control law. For the energy harvesting systems presented in this paper, the Lyapunov equation used to determine the nonlinear control law also decouples, which results in only half of the system states needed for the control law. The main result of this study is that more average power can be harvested with the electronics implementing the optimal control law or the sub-optimal, nonlinear control law than by implementing the optimal static admittance. This result is illustrated for both the electromagnetic and piezoelectric energy harvesters through the unconstrained and constrained $\bar{P}_{gen}$ ratios.

ACKNOWLEDGMENTS

Work by the first two authors was supported by NSF award CMMI-0747563. The views expressed in this article are those of the authors, and do not necessarily reflect those of the National Science Foundation.

REFERENCES

[1] Roundy, S., Wright, P. K., and Rabaey, J., 2002. "A study of low level vibrations as a power source for wireless sensor nodes". Journal of Computer Communications, **26**, pp. 1131–1144.

[2] Beeby, S. P., Tudor, M. J., and White, N. M., 2006. "Energy harvesting vibration sources for microsystems applications". Measurement Science and Technology, **17**, pp. R175–R195.

[3] Knight, C., Davidson, J., and Behrens, S., 2008. "Energy options for wireless sensor nodes". Sensors, **8**, pp. 8037–8066.

[4] Kasyap, A., Lim, J., Johnson, D., Horowitz, S., Nishida, T., Ngo, K., Sheplak, M., and Cattafesta, L., 2002. "Energy reclamation from a vibrating piezoceramic composite beam". In Ninth Interational Congress on Sound and Vibration.

[5] Lefeuvre, E., Audigier, D., Richard, C., and Guyomar, D., 2007. "Buck-boost converter for sensorless power optimization of piezoelectric energy harvester". IEEE Transactions on Power Electronics, **22**, pp. 2018–2025.

[6] Kong, N., Ha, D. S., Erturk, A., and Inman, D., 2010. "Resistive impedance matching circuit for piezoelectric energy harvesting". Journal of Intelligent Material Systems and Structures. in press.

[7] Scruggs, J. T., 2010. "On the causal power generation limit for a vibratory energy harvester in broadband stochastic response". Journal of Intelligent Material Systems and Structures, **21**, pp. 1249–1262.

[8] Ottman, G. K., Hofmann, H. F., and Lesieutre, G. A., 2003. "Optimized piezoelectric energy harvesting circuit using step-down converter in discontinuous conduction mode". IEEE Transactions On Power Electronics, **18**, pp. 696–703.

[9] Stephen, N. G., 2006. "On energy harvesting from ambient vibration". Journal of Sound and Vibration, **293**, pp. 409–425.

[10] Adhikari, S., Friswell, M., and Inman, D., 2009. "Piezoelectric energy harvesting from broadband random vibrations". Smart Materials and Structures, **18**. AN 115005.

[11] Kassakian, J., Schlecht, M., and Verghese, G., 1991. Principles of Power Electronics. Addison-Wesley, Reading, MA.

[12] Scruggs, J. T., and Cassidy, I. L., 2010. "Optimal and sub-optimal power management in broadband vibratory energy harvesters with one-directional power flow constraints". In SPIE International Symposium on Smart Materials and Structures/NDE.

[13] Brogliato, B., Lozano, R., Maschke, B., and Egeland, O., 2007. Dissipative Systems Analysis and Control. Springer-Verlag, London.

[14] Lozano-Leal, R., and Joshi, S., 1988. "On the design of dissipative lqg type controller". In IEEE Conference on Decision and Control.

[15] Ward, J. K., and Behrens, S., 2008. "Adaptive learning algorithms for vibration energy harvesting". Smart Materials and Structures, **17**, p. 17:035025.

[16] Glynne-Jones, P., Tudor, M. J., Beeby, S. P., and White, N. M., 2004. "An electromagnetic, vibration-powered generator for intelligent sensor systems". Sensors and Actuators, **A 110**, pp. 344–349.

[17] Cassidy, I. L., Scruggs, J. T., and Behrens, S., 2011. "Optimization of partial-state feedback for vibratory energy harvesters subjected to broadband stochastic disturbances". Smart Materials and Structures. Submitted.

[18] Scruggs, J. T., Taflanidis, A. A., and Iwan, W. D., 2007. "Nonlinear stochastic controllers for semiactive and regenerative systems yielding guaranteed quadratic performance bounds. part 1: State feedback control". Journal of Structural Control and Health Monitoring, **14**, pp. 1101–1120.